

THE LOW QUIESCENT X-RAY LUMINOSITY OF THE TRANSIENT X-RAY BURSTER EXO 1747–214

JOHN A. TOMSICK¹, DAWN M. GELINO², PHILIP KAARET³

Draft version September 29, 2018

ABSTRACT

We report on X-ray and optical observations of the X-ray burster EXO 1747–214. This source is an X-ray transient, and its only known outburst was observed in 1984–1985 by the *EXOSAT* satellite. We re-analyzed the *EXOSAT* data to derive the source position, column density, and a distance upper limit using its peak X-ray burst flux. We observed the EXO 1747–214 field in 2003 July with the *Chandra X-ray Observatory* to search for the quiescent counterpart. We found one possible candidate just outside the *EXOSAT* error circle, but we cannot rule out the possibility that the source is unrelated to EXO 1747–214. Our conclusion is that the upper limit on the unabsorbed 0.3–8 keV luminosity is $L < 7 \times 10^{31}$ erg s⁻¹, making EXO 1747–214 one of the faintest neutron star transients in quiescence. We compare this luminosity upper limit to the quiescent luminosities of 19 neutron star and 14 black hole systems and discuss the results in the context of the differences between neutron stars and black holes. Based on the theory of deep crustal heating by Brown and coworkers, the luminosity implies an outburst recurrence time of >1300 yr unless some form of enhanced cooling occurs within the neutron star. The position of the possible X-ray counterpart is consistent with three blended optical/IR sources with *R*-magnitudes between 19.4 and 19.8 and *J*-magnitudes between 17.2 and 17.6. One of these sources could be the quiescent optical/IR counterpart of EXO 1747–214.

Subject headings: accretion, accretion disks — stars: neutron — stars: individual (EXO 1747–214) — X-rays: stars — X-rays: general

1. INTRODUCTION

Observations of transient X-ray binary systems in quiescence have greatly advanced studies of compact objects over the past decade. While both black hole and neutron star systems can approach or possibly even exceed their Eddington luminosities during outbursts, their quiescent X-ray luminosities can be factors of $>10^7$ lower than their peak luminosities. Quiescent optical observations allow for the measurement of compact object masses as the optical companion’s radial velocity curves can be measured as well as the binary inclination via studies of ellipsoidal modulations (Charles & Coe 2003, and references therein). Such measurements have been especially important for confirming that there is a population of compact objects with masses that are too high ($>3M_{\odot}$) to be neutron stars so that these objects are very likely black holes. In the future, mass measurements of neutron star transients may lead to constraints on the equation of state for matter at high densities (Lattimer & Prakash 2004).

Quiescent X-ray observations are also interesting for neutron star and black hole systems. For many neutron star systems, a thermal component is seen in the quiescent X-ray spectrum that is likely blackbody emission from the neutron star surface. Measurements of the evolution of this component allow for constraints on the thermal properties of the neutron star crust and core (Wijnands 2004). The core temperature is thought to be set by the accretion history over a time period of 10,000 years (Brown, Bildsten & Rutledge 1998; Colpi et al. 2001). Quiescent X-ray spectra of black hole systems do not appear to show a blackbody component, which is one reason they tend to be fainter than neutron star

systems. It has also been argued that, in quiescence, black holes are radiatively less efficient than neutron star systems, which has been taken as evidence that a large fraction of the accreted matter is advected across the black hole event horizon (Narayan, Garcia & McClintock 1997; McClintock et al. 2003).

With sensitive X-ray missions like the *Chandra X-ray Observatory* and the *X-ray Multi-Mirror Mission (XMM-Newton)*, it has been possible to observe many more neutron star and black hole systems in quiescence. As more systems are observed, it has been found that many of the neutron star systems are fainter than the 10^{32-34} erg s⁻¹ range usually considered as the typical range for neutron stars in quiescence (Campana et al. 2002; Wijnands et al. 2005b; Tomsick et al. 2004; Jonker, Wijnands & van der Klis 2004). Thus, it is important to obtain the largest samples possible to avoid any selection biases when comparing the quiescent properties of black holes and neutron stars.

In this paper, we use archival data as well as our recent observations to study the neutron star X-ray transient EXO 1747–214. This system was discovered during the *EXOSAT* Galactic plane scans in 1984 June (Warwick et al. 1988; Parmar et al. 1985) and was detected again by *EXOSAT* in 1985 April at about the same flux level (Magnier et al. 1989; Parmar et al. 1985). These are the only two known detections of the source, so that it has apparently been in quiescence for 20 years. An X-ray burst was detected in 1985, demonstrating that the system definitely harbors a neutron star (Magnier et al. 1989). Although *EXOSAT* provided a relatively good 15'' position for the source, and the extinction along the line of sight to the source ($l = 7^{\circ}.00, b = +2^{\circ}.95$) is fairly low, the source has not been optically identified. The primary goal of this work is to use a *Chandra* observation of moderate length to detect the source in quiescence and to search for an optical counterpart. We report on our search below, including a constraint on the quiescent luminosity and a comparison between the Eddington-scaled luminosity of

arXiv:astro-ph/0509109v1 6 Sep 2005

¹ Center for Astrophysics and Space Sciences, Code 0424, University of California at San Diego, La Jolla, CA, 92093 (e-mail: jtomsick@ucsd.edu)

² Michelson Science Center, California Institute of Technology, 770 South Wilson Avenue, MS 100-22, Pasadena, CA 91125

³ Department of Physics and Astronomy, University of Iowa, Iowa City, IA 52242

EXO 1747–214 and those of 19 neutron star and 14 black hole systems.

2. ANALYSIS AND RESULTS

The data we used for this work come from the X-ray, optical, and infrared observations listed in Table 1. First, we went back to the discovery observations made by *EXOSAT* in 1984–1985. During this time, the source was bright in X-rays, and we used the *EXOSAT* images to re-derive the source position. We also re-analyzed the data from the *EXOSAT* proportional counters to obtain information about the energy spectrum and the detected X-ray burst. The main focus of this paper is to search for the quiescent X-ray counterpart. For this purpose, we used the data from our 2003 *Chandra* observation. Finally, we obtained optical and infrared images to allow for optical or IR identifications of any detected X-ray sources. Here, we describe our analysis of the data from these observations and our results.

2.1. Source Position from EXOSAT

EXOSAT (Taylor et al. 1981) observations of EXO 1747–214 occurred in 1985 on April 8 and 11. The most precise position for this source comes from data obtained with the low energy imaging telescope (LE1) and the Channel Multiplier Array (CMA1) instrument, which has a bandpass of 0.05–2.5 keV. However, as the *EXOSAT/CMA* catalog⁴ does not give a single unique position for EXO 1747–214, we re-analyzed the CMA data to determine the position. During the short April 8 observation, the Thin Lexan filter was inserted, and EXO 1747–214 was $\sim 6'$ off-axis. On April 11, the source was on-axis, and three filters were used at different times: Thin Lexan, with the highest effective area (A_{eff}) over the full bandpass; Al/Parylene, with reduced A_{eff} below 0.3 keV; and Boron, with two bands of A_{eff} peaking at 0.15 keV and 1 keV (de Korte et al. 1981). With the highest A_{eff} and the longest exposure time (see Table 1), the image obtained with the Thin Lexan filter provides the best statistics, and this image is shown in Figure 1. Nearly all of the source counts are contained in a 24-by-24 pixel region centered on the source. For the image shown in Figure 1, there are 1331 counts in this region, and using number of counts per pixel from the surrounding, source-free, region, we estimate that there are 104 background counts in a 24-by-24 pixel region. For each of the four images, we calculated the centroid using the counts from a 24-by-24 pixel region centered on the source, and these centroids are shown in Figure 1. The position on April 8 is $\sim 10''$ away from the other three positions, and this is probably due to the fact that the source was off-axis on April 8 so that the position is not as reliable. We combined the data for the three on-axis images and recalculated the centroid to determine a best source position of R.A. = $17^{\text{h}}50^{\text{m}}25^{\text{s}}.8$, decl. = $-21^{\circ}25'22''$ (equinox J2000). The *EXOSAT/CMA* catalog indicates that the 90% confidence error radius is $15''$, and the corresponding error circle is shown in Figure 1. The best position that we derive is $4''.5$ from the median of the positions given in the *EXOSAT/CMA* catalog, and it is $2''.8$ from the position quoted in Gottwald et al. (1991). Thus, all these positions are well within the $15''$ error circle.

2.2. Column Density and Distance Upper Limit from EXOSAT

⁴ The *EXOSAT/CMA* catalog is part of the “Master X-Ray Catalog” at <http://heasarc.gsfc.nasa.gov/W3Browse/all/xray.html>

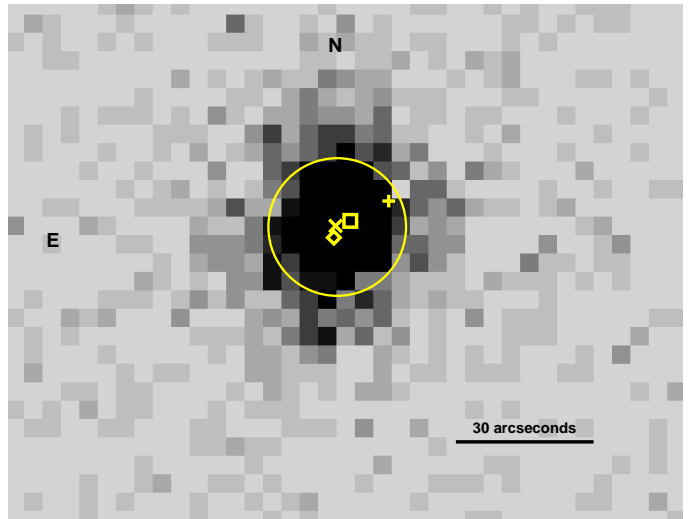


FIG. 1.— The 0.05–2.5 keV image of EXO 1747–214 in outburst. The data come from the *EXOSAT* CMA instrument. The observation occurred on 1985 April 11, and the exposure time was 9,171 s. The $15''$ radius circle shows the 90% confidence (including systematic pointing errors) *EXOSAT* error region for EXO 1747–214. The cross, the diamond, and the square show the positions derived from data taken with the three CMA filters on 1985 April 11. The plus marks the position obtained from the observation made on 1985 April 8.

On 1985 April 11, EXO 1747–214 was also observed with the *EXOSAT* medium energy (ME) instrument, which consists of eight proportional counters. The observation lasted for more than 6 hours, and, as reported in Magnier et al. (1989), included one type I X-ray burst. The original analysis by Magnier et al. (1989) reported that the 1–20 keV spectrum of the persistent emission was well-described by a power-law with interstellar absorption with a column density of $N_{\text{H}} = 1 \times 10^{22} \text{ cm}^{-2}$. To check this, we obtained the ME spectrum from the *EXOSAT* archive. The details of the spectral extraction and background subtraction are provided on-line⁵. When the EXO 1747–214 spectrum was extracted, the data from the time of the X-ray burst was removed, leaving the spectrum of the persistent emission.

We used the spectral fitting package XSPEC version 11.3.1t to perform least-squares fits to the ME spectrum, and our results do not confirm those of Magnier et al. (1989). A power-law with (interstellar) absorption gives a very poor fit to the spectrum with $\chi^2/\nu = 498/28$. The reason for the poor fit is that the spectrum drops more rapidly at high energies than a power-law model, indicating the presence of a cutoff. Models that include a cutoff greatly improve the fit. An exponentially cutoff power-law (“cutoffpl” in XSPEC) with absorption gives $\chi^2/\nu = 68/27$ and a much lower column density than $1 \times 10^{22} \text{ cm}^{-2}$. A Comptonization model (“comptt” in XSPEC) with absorption gives a statistically acceptable fit with $\chi^2/\nu = 26/26$. The spectrum fitted with a Comptonization model is shown in Figure 2. With this fit, the column density, using Anders & Grevesse (1989) abundances and Balucinska-Church & McCammon (1992) cross-sections, is $N_{\text{H}} = (1.9^{+2.8}_{-1.9}) \times 10^{21} \text{ cm}^{-2}$ (90% confidence errors), which is consistent with the Galactic value of $4.0 \times 10^{21} \text{ cm}^{-2}$ (Dickey & Lockman 1990). We fixed N_{H} to the Galactic value and re-fitted the 1–20 keV spectrum. The Comptoniza-

⁵ <http://heasarc.gsfc.nasa.gov/W3Browse/exosat/me.html>

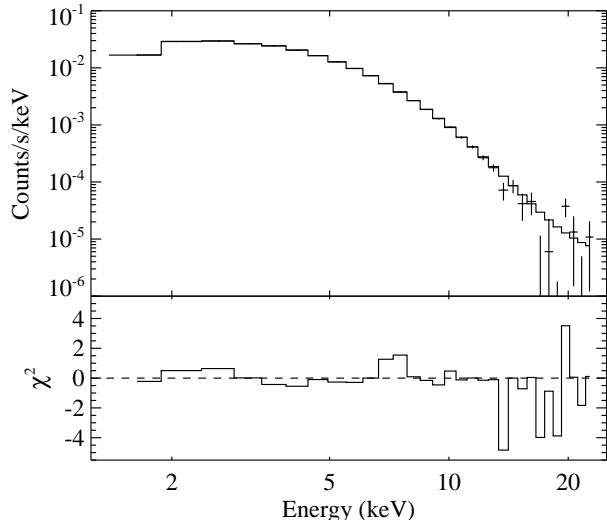


FIG. 2.— The *EXOSAT* ME energy spectrum from a 22,450 s observation made on 1985 April 11. The spectrum is fitted with a Comptonization (“comptt”) model and interstellar absorption with N_{H} fixed at the Galactic value of $4 \times 10^{21} \text{ cm}^{-2}$. The fitted “comptt” parameter values include: The temperature of the “seed” photons, $0.34 \pm 0.02 \text{ keV}$; the plasma temperature, $2.17 \pm 0.06 \text{ keV}$; and the optical depth of the plasma, 7.0 ± 0.2 . The data and model are shown in the top panel, and the residuals are shown in the bottom panel. We measure a 1–20 keV flux of $1.45 \times 10^{-9} \text{ erg cm}^{-2} \text{ s}^{-1}$.

tion parameters from this fit are given in the caption of Figure 2. Below, we assume that the interstellar column density is at the Galactic value.

We use the fact that the peak X-ray burst flux must be below the Eddington luminosity to derive an upper limit on the distance to EXO 1747–214. To derive the peak flux, we use the X-ray burst spectral results from Magnier et al. (1989) and the peak 1–8 keV count rate of 2343 c/s, which we obtain from our re-analysis of the *EXOSAT* data. Fitting spectra around the peak of the burst with 0.5 s time resolution with a blackbody model, Magnier et al. (1989) find that the peak burst temperature is $\sim 2 \text{ keV}$. After fixing the temperature to 2 keV and assuming $N_{\text{H}} = 4 \times 10^{21} \text{ cm}^{-2}$, we adjusted the blackbody normalization to give the peak 1–8 keV count rate. This leads to an unabsorbed 1–20 keV flux of $2.7 \times 10^{-8} \text{ erg cm}^{-2} \text{ s}^{-1}$. For radius expansion bursts from neutron stars in globular clusters (i.e., Eddington limited bursts from neutron stars at known distances), Kuulkers et al. (2003) found an average peak luminosity of $3.8 \times 10^{38} \text{ erg s}^{-1}$. From this luminosity and the peak flux of the EXO 1747–214 burst, we derive a distance upper limit of $d < 11 \text{ kpc}$.

2.3. A Search for the Quiescent X-Ray Counterpart with Chandra

We obtained a 24.5 ks *Chandra* observation of the EXO 1747–214 field on 2003 July 31 (Observation ID 3802). We used the Advanced CCD Imaging Spectrometer (ACIS, Garmire et al. 2003) with the target position placed on one of the back-illuminated ACIS chips (ACIS-S3). For our observation, the instrument was in the “VFaint” mode, which provides the maximum information about each event and thus, the best rejection of background events. We started with the “level 1” event list produced by the standard data processing with ASCDS version 6.13.4 and performed further processing using the *Chandra* Interactive Analysis of Obser-

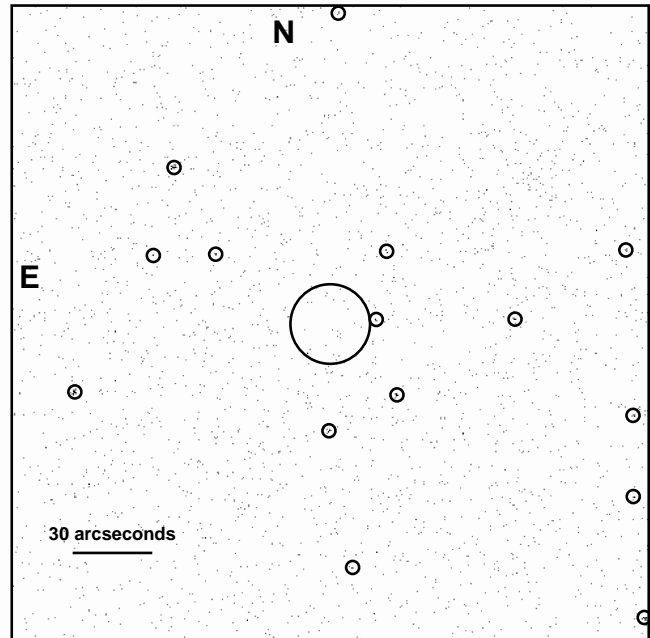


FIG. 3.— The 0.3–8 keV *Chandra*/ACIS image of the EXO 1747–214 field. The exposure time is 24.5 ks, and the image size is 4'–by–4'. The 15'' radius circle shows the 90% confidence *EXOSAT* error circle for EXO 1747–214. The other 15 circles mark the detected *Chandra* sources.

vations (CIAO) version 3.2 software and Calibration Data Base (CALDB) version 3.0.1. We used the CIAO routine *acis_process_events* to obtain a “level 2” event list and image, and we searched for sources using this image.

For our source search, we focused on a 4'–by–4' square region of the ACIS-S3 chip centered on the *EXOSAT* position. We restricted the energy range to 0.3–8 keV and used the CIAO routine *wavdetect* (Freeman et al. 2002) to search for sources. Based on the image size of 488-by-488 pixels and our detection threshold of 4.2×10^{-6} , we would expect to detect ~ 1 spurious source. We detected 15 sources ranging from 3 to 24 counts. Using the background estimates generated by *wavdetect* and Poisson statistics, the 3 and 4 count sources are detected at significances of $\sim 3.5\text{-}\sigma$ and $\sim 4.1\text{-}\sigma$, respectively. Figure 3 shows the *Chandra* image with the 15 sources circled. The 15'' 90% confidence *EXOSAT* error circle is also shown. None of the *Chandra* sources fall within the error circle, and only one of the sources lies close enough (17''.5 away) to be considered a possible quiescent counterpart to EXO 1747–214. The position of this possible counterpart, which is one of the sources with 4 counts, is R.A. = $17^{\text{h}}50^{\text{m}}24^{\text{s}}.52$, decl. = $-21^{\circ}25'19''.9$ (equinox J2000, 0''.6 uncertainty). Given the density of sources that we detect (15 sources in a 16 arcmin^2 region), the probability of finding a source within 17''.5 of the best EXO 1747–214 position by chance is 19%. Thus, the possible counterpart could be an unrelated X-ray source.

Although the $3\text{-}\sigma$ detection threshold for the *EXOSAT* error region is close to 3 counts, considering the possible 4 count source just outside the *EXOSAT* error circle, the most concise statement of our results is that the number of 0.3–8 keV counts from the quiescent EXO 1747–214 counterpart is ≤ 4 . This corresponds to a limit on the 0.3–8 keV count rate of $\leq 1.63 \times 10^{-4} \text{ c/s}$. To determine what this implies in terms of

the source flux and luminosity, we used the CIAO tools to produce an ACIS response matrix for this observation. To calculate the flux upper limit, we assumed $N_{\text{H}} = 4 \times 10^{21} \text{ cm}^{-2}$ and several different spectral models that are similar to the typical X-ray spectra of quiescent neutron star systems, including a thermal model, a non-thermal model, and a two-component model. For the thermal model, we used a neutron star atmosphere model (“nsa” in XSPEC, Zavlin, Pavlov & Shibano 1996) and assumed a source distance of 11 kpc (the upper limit), a neutron star mass of $1.4 M_{\odot}$, and a neutron star radius of 10 km. The only other free parameter in the model is the temperature (kT_{eff}). We adjusted kT_{eff} to make the predicted count rate match the upper limit given above, and this occurs at 63 eV. For this model, the absorbed 0.3–8 keV flux is $5.6 \times 10^{-16} \text{ erg cm}^{-2} \text{ s}^{-1}$ and the unabsorbed flux is $4.9 \times 10^{-15} \text{ erg cm}^{-2} \text{ s}^{-1}$. Non-thermal power-law models with photon indices of $\Gamma = 2$ and 3 give upper limits on the unabsorbed flux of 2.5×10^{-15} and $3.6 \times 10^{-15} \text{ erg cm}^{-2} \text{ s}^{-1}$, respectively. We also considered two-component, nsa plus power-law, models with $kT_{\text{eff}} = 55 \text{ eV}$ along with the same nsa parameters as above. For photon indices of $\Gamma = 1$ and 2, the upper limits on the unabsorbed flux are 4.2×10^{-15} and $3.9 \times 10^{-15} \text{ erg cm}^{-2} \text{ s}^{-1}$, respectively. In summary, the highest flux is obtained using the pure thermal model. Using this flux ($4.9 \times 10^{-15} \text{ erg cm}^{-2} \text{ s}^{-1}$) along with the fact that $d < 11 \text{ kpc}$, we conclude that $L < 7 \times 10^{31} \text{ erg s}^{-1}$ (0.3–8 keV).

2.4. Optical and Infrared Observations

A couple of months after the *Chandra* observation, we obtained a deep *R*-band image of the EXO 1747–214 field at Keck Observatory. For the single 600 s image, we performed bias subtraction and flat-fielding in the standard manner using IRAF⁶. To register the image, we identified six of the stars in the image with stars in the USNO-B catalog, and used IRAF routines to calculate the sky projection. For magnitude calibration, we obtained observations of Landolt (1992) standards PG 1657+078 and PG 0231+051 before and after observing the EXO 1747–214 field and performed aperture photometry for the standard stars as well as for several stars in the EXO 1747–214 field. Figure 4 shows the central part of the Keck image, including the EXO 1747–214 error circle and the possible *Chandra* counterpart described above. The possible counterpart is positionally coincident with three blended optical sources as shown in the figure. The three optical sources are approximately the same brightness, and all three are in the $R = 19.4$ – 19.8 range.

We also obtained an infrared *J*-band image of the EXO 1747–214 field in 2002. We used the 4 meter telescope at Cerro Tololo Inter-American Observatory (CTIO) along with the Optical System for Imaging and Low-Resolution Integrated Spectroscopy (OSIRIS) instrument. We detect the three optical sources discussed above, and all three are in the $J = 17.2$ – 17.6 range.

While this positional coincidence certainly does not prove that this source is the EXO 1747–214 counterpart, it is notable that the properties of the optical sources are consistent with what might be expected for the EXO 1747–214 counterpart. The sources appear to be point-like as opposed to being extended as might be the case if they are galaxies. Also, the

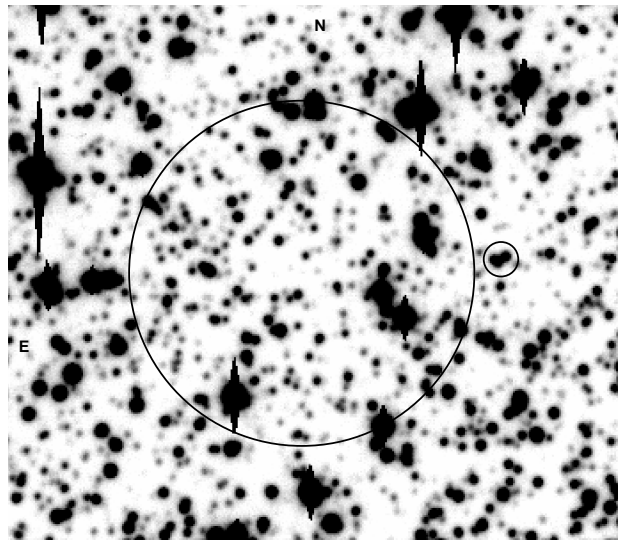


FIG. 4.— A 600 s *R*-band image taken using the ESI instrument at Keck Observatory. The large circle sets the scale and is the $15''$ 90% confidence *EXOSAT* error circle for EXO 1747–214. The smaller circle marks the location of a four count *Chandra* source. Its position is consistent with any of the three $R = 19.4$ – 19.8 optical sources in the smaller circle.

magnitude range is not unreasonable for a quiescent neutron star LMXB at a few kpc. For $R = 19.6$, $A_R = 1.7$, and $d = 3 \text{ kpc}$, the absolute magnitude is $M_R = 5.5$, which is consistent with a K3V or K4V star. In addition, a *J*-magnitude of 17.4 and $A_J = 0.6$ indicate a de-reddened R – J color of 1.1, which is also consistent with main sequence K-type star. If the possible counterparts have spectra consistent with those of main sequence stars, then they are not at a distance that is much more than a few kpc. For example, the *R*-band measurement and a distance of 11 kpc imply $M_R = 2.7$ and a late-F spectral type, but the R – J colors are not consistent with an F-type star (even considering the range of measured *R* and *J*-magnitudes).

3. DISCUSSION

3.1. Neutron Star/Black Hole Comparison

The upper limit on the EXO 1747–214 X-ray luminosity of $7 \times 10^{31} \text{ erg s}^{-1}$ (0.3–8 keV) places it among the faintest of the quiescent neutron star systems. One reason that faint neutron star systems are of interest is that claims for the existence of black hole event horizons rely on the faintness of black hole systems relative to neutron star systems (Narayan, Garcia & McClintock 1997; Menou et al. 1999; Garcia et al. 2001; McClintock et al. 2003). The faintness of the black hole systems may be due to advection of accretion energy across the event horizon as occurs in Advection-Dominated Accretion Flow (ADAF) models (Narayan, Garcia & McClintock 1997, and references therein) or to the lack of the thermal component that is often present for quiescent neutron star systems. In either case, one interpretation for the difference is that neutron stars have a solid surface while black holes do not.

To place our EXO 1747–214 luminosity upper limit in the context of this discussion, we compiled a list of 14 black hole and 20 (including EXO 1747–214) neutron star transients with constraints on the quiescent luminosity (L_{min}). The black hole list is complete in the sense that it includes all confirmed black hole systems for which sensitive quiescent X-ray observations have been made. In all, there are 17 dynamically con-

⁶ IRAF (Image Reduction and Analysis Facility) is distributed by the National Optical Astronomy Observatories, which are operated by the Association of Universities for Research in Astronomy, Inc., under cooperative agreement with the National Science Foundation.

firmed black hole systems (McClintock & Remillard 2003; Casares et al. 2004; Orosz et al. 2004). Only GRS 1915+105, XTE J1650–500, and GS 1354–64 do not have quiescent X-ray coverage. We compiled the list of neutron star transients from the recent literature, including papers where neutron star sub-populations were studied (e.g., Jonker et al. 2004; Tomsick et al. 2004; Garcia et al. 2001). Our list is nearly complete for field systems, but we only included the best studied globular cluster systems (see Heinke et al. 2003, for additional globular cluster sources).

In previous work (e.g., Garcia et al. 2001), it has been argued that, for a black hole or neutron star system with a given orbital period (P_{orb}), the Eddington-scaled mass accretion rate would be expected to be the same for black hole and neutron star systems. If this is true, the Eddington-scaled X-ray luminosity is the best parameter for comparing the sources. We calculated $L_{\text{min}}/L_{\text{Edd}}$ for our list of systems, and the values are shown in Figure 5. For the black hole systems, the luminosities come from Tomsick et al. (2003) and references therein, and the black hole masses and errors on the masses come from Charles & Coe (2003). The neutron star luminosities come from the references shown in the Figure 5 caption. To determine the errors on $L_{\text{min}}/L_{\text{Edd}}$, we assume for all systems that the unabsorbed soft X-ray fluxes are measured to an accuracy of 40% and that the distances are known to 25%. The assumed errors are not exactly correct for all sources, but they represent values that are typically quoted in the literature. While the black hole errors also include a contribution from the uncertainty in the black hole mass, we assume that all the neutron stars have masses of $1.4 M_{\odot}$. The bandpasses for the luminosities are nearly the same being 0.3–8 keV, 0.3–7 keV, or 0.5–10 keV in all cases. It is important to keep in mind that we are only quoting the X-ray luminosities here and that bolometric corrections could be important. The sources in Figure 5 are ordered according to orbital period in cases for which P_{orb} is known.

The $\log_{10}(L_{\text{min}}/L_{\text{Edd}})$ values shown in Figure 5 indicate that the black holes are, on average, fainter. For black holes, the median luminosity is a factor of 42 lower than for neutron stars. While part of this effect is due to the higher black hole masses, the average black hole mass is $7.7 M_{\odot}$, which is only a factor of 5.5 higher than the neutron star masses assumed. Currently, the only clear overlap between the distributions is caused by the high luminosity of V404 Cyg, and as this source has the longest orbital period and has an evolved optical companion, this may be due to a higher quiescent mass accretion rate for V404 Cyg. However, several of the neutron star systems, including EXO 1747–214, have upper limits that are approaching the values seen for some of the other black hole systems. It is important to determine how faint sources like EXO 1747–214 and 3A 1905+000 (Juett & Chakrabarty 2005) are (as well as their orbital periods) as the neutron star and black hole distributions could significantly overlap in contradiction to what is expected for accretion models that include black hole advection such as the ADAF model.

3.2. Neutron Star Cooling

One reason that EXO 1747–214 may be so faint is that, as far as we know, it has been in quiescence for 20 years. Based on the theory of deep crustal heating for transient neutron stars (Brown, Bildsten & Rutledge 1998), the evolution of the X-ray flux in the thermal component between outbursts depends on the source’s mass accretion (and thus outburst) history. Rutledge et al. (2002) show that for a long (13 year)

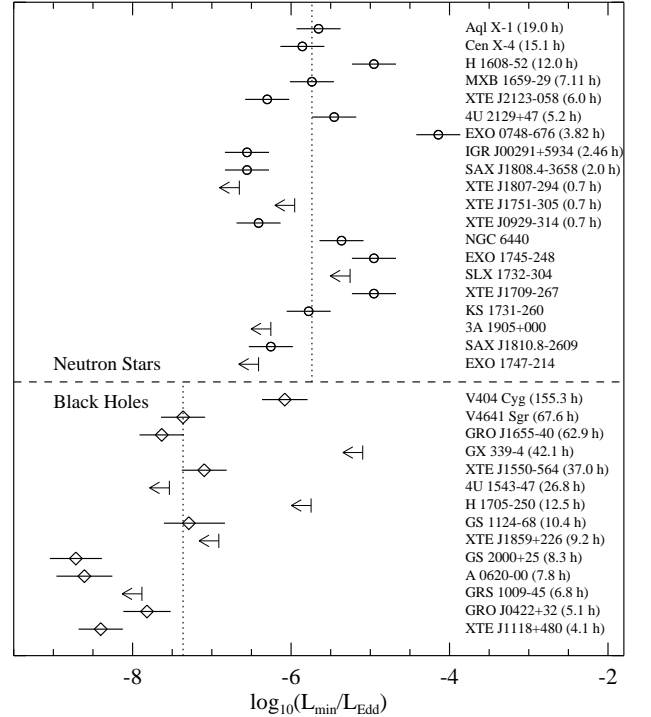


FIG. 5.— The Eddington-scaled minimum X-ray luminosities for neutron star and black hole transients. The bandpasses for the luminosities (which are unabsorbed) are nearly the same in each case (0.3–8 keV, 0.3–7 keV, or 0.5–10 keV). The selection criteria and the description of how we calculated the values are described in detail in § 3.1. The black hole luminosities come from Tomsick et al. (2003) and references therein, and the neutron star luminosities come from the following: Garcia et al. (2001); Jonker et al. (2004); Jonker, Wijnands & van der Klis (2004); Campana et al. (2002, 2005); Tomsick et al. (2004); Juett & Chakrabarty (2005); Wijnands, Heinke & Grindlay (2002); Wijnands et al. (2001, 2004, 2005b,a); Cackett et al. (2005). For sources with measured orbital periods, P_{orb} is given in parentheses after the source name. The vertical dotted lines mark the median Eddington-scaled luminosities.

outburst, the temperature of the crust can rise significantly, and it can take years or decades (depending on the conductivity of the crust and the type of neutrino cooling that occurs) for the crust to reach thermal equilibrium. At that point, the source will reach its lowest luminosity at a level set by the temperature of the neutron star’s core, which depends on the mass accretion rate over a 10,000 year time scale (Colpi et al. 2001).

To some extent, the X-ray coverage in the 1980s limits our knowledge of the EXO 1747–214 outburst history. Historically, the source has only been detected by *EXOSAT*, and it was detected in 1984 June and 1985 April. In both cases, the persistent X-ray flux was near 10^{-9} erg cm $^{-2}$ s $^{-1}$. The missions with all-sky coverage in that era were *Ariel V*, which lasted until 1980 and *Ginga* which began in 1987 (Chen, Shrader & Livio 1997). The 90% sky coverage from *Tenma* during 1983–1984 make it unlikely that the EXO 1747–214 outburst started much before 1984 June. Thus, assuming that EXO 1747–214 had a single outburst, its duration was very likely between 10 months and ~ 3 years. For the 13 year outburst from KS 1731–260, Rutledge et al. (2002) find that the neutron star cooling is dominated by the core rather than the crust 1 year after the outburst for a high-conductivity crust and 30 years after the outburst for

a low-conductivity crust. Given the shorter duration of the EXO 1747–214 outburst, it is likely that EXO 1747–214 was in the core-dominated phase when the *Chandra* observation occurred.

We can calculate the outburst recurrence time predicted by the Brown, Bildsten & Rutledge (1998) theory for EXO 1747–214. The recurrence time is given by $t_{\text{rec}} = (t_{\text{otb}}/130)(F_{\text{otb}}/F_{\text{q}})$ (Wijnands et al. 2001; Tomsick et al. 2004), where t_{otb} and F_{otb} are the outburst duration and average flux level during the outburst, respectively, and F_{q} is the quiescent flux level. Assuming an outburst duration of 10 months (at the lower end of the range derived above) and an average outburst flux of 10^{-9} erg cm $^{-2}$ s $^{-1}$, the upper limit on the quiescent flux of 5×10^{-15} erg cm $^{-2}$ s $^{-1}$ implies that $t_{\text{rec}} > 1300$ years. If, in the future, it is found that the recurrence time is in fact shorter than this value, then a mechanism for enhanced cooling of the core would be necessary.

4. CONCLUSIONS AND FUTURE WORK

EXO 1747–214 is one of several neutron star systems with a quiescent luminosity that is lower than the typical 10^{32-34} erg s $^{-1}$ range. Our *Chandra* observation indicates a 0.3–8 keV luminosity upper limit of $L < 7 \times 10^{31}$ erg s $^{-1}$. In the *Chandra* image, there is only one source that is a possible EXO 1747–214 quiescent counterpart. The source is detected at a significance level of $4.1\text{-}\sigma$, leaving a small chance that it is spurious, and it is just outside the 90% confidence *EXOSAT* error circle. Overall, we cannot rule out the possibility that the source is unrelated to EXO 1747–214. Our optical and IR images show that the position of this possible counterpart is consistent with three blended optical/IR sources with *R*-band magnitudes be-

tween 19.4 and 19.8 and *J*-band magnitudes between 17.2 and 17.6. If one of these is the EXO 1747–214 counterpart, it would imply a distance of a few kpc, significantly lower than the 11 kpc upper limit derived from the peak X-ray burst flux. This, in turn, would imply a significantly lower quiescent X-ray luminosity.

As EXO 1747–214 is one of the faintest (if not the faintest of the) neutron star transients in quiescence, it is important to obtain deeper X-ray observations to determine the actual quiescent flux. This is important for studies of neutron star cooling as well as the comparison between the quiescent radiative efficiency of black hole vs. neutron star sources. Another avenue for further study is to obtain optical spectra of the candidate counterparts. For example, detecting an H α emission line would be a strong X-ray binary indicator. Finally, it is worth pointing out that finding the optical counterpart is likely the only way that we will be able to improve the determination of the source distance.

JAT would especially like to thank L. Angelini for assistance with using the data in the *EXOSAT* archive and G. Tovmassian for useful discussions. JAT acknowledges partial support from *Chandra* award number GO3-4041X issued by the *Chandra* X-ray Observatory Center, which is operated by the Smithsonian Astrophysical Observatory for and on behalf of NASA under contract NAS8-03060. Data for this work were obtained at the W.M. Keck Observatory, which is operated as a scientific partnership among the University of California, Caltech and NASA. The SIMBAD database and the HEASARC Data Archive were used in preparing this paper.

REFERENCES

- Anders, E., & Grevesse, N., 1989, *Geochimica et Cosmochimica Acta*, 53, 197
- Balucinska-Church, M., & McCammon, D., 1992, *ApJ*, 400, 699
- Brown, E. F., Bildsten, L., & Rutledge, R. E., 1998, *ApJ*, 504, L95
- Cackett, E. M., et al., 2005, *ApJ*, 620, 922
- Campana, S., Ferrari, N., Stella, L., & Israel, G. L., 2005, *A&A*, 434, L9
- Campana, S., et al., 2002, *ApJ*, 575, L15
- Casares, J., Zurita, C., Shahbaz, T., Charles, P. A., & Fender, R. P., 2004, *ApJ*, 613, L133
- Charles, P. A., & Coe, M. J., 2003, Review Article, *astro-ph/0308020*
- Chen, W., Shrader, C. R., & Livio, M., 1997, *ApJ*, 491, 312
- Colpi, M., Geppert, U., Page, D., & Possenti, A., 2001, *ApJ*, 548, L175
- de Korte, P. A. J., et al., 1981, *Space Science Reviews*, 30, 495
- Dickey, J. M., & Lockman, F. J., 1990, *ARA&A*, 28, 215
- Freeman, P. E., Kashyap, V., Rosner, R., & Lamb, D. Q., 2002, *ApJS*, 138, 185
- Garcia, M. R., McClintock, J. E., Narayan, R., Callanan, P., Barret, D., & Murray, S. S., 2001, *ApJ*, 553, L47
- Garmire, G. P., Bautz, M. W., Ford, P. G., Nousek, J. A., & Ricker, G. R., 2003, in *X-Ray and Gamma-Ray Telescopes and Instruments for Astronomy*. Edited by Joachim E. Truemper, Harvey D. Tananbaum. Proceedings of the SPIE, 4851, 28
- Gottwald, M., Steinle, H., Pietsch, W., & Graser, U., 1991, *A&AS*, 89, 367
- Heinke, C. O., Grindlay, J. E., Lloyd, D. A., & Edmonds, P. D., 2003, *ApJ*, 588, 452
- Jonker, P. G., Galloway, D. K., McClintock, J. E., Buxton, M., Garcia, M., & Murray, S., 2004, *MNRAS*, 354, 666
- Jonker, P. G., Wijnands, R., & van der Klis, M., 2004, *MNRAS*, 349, 94
- Juett, A. M., & Chakrabarty, D., 2005, *ApJ*, 627, 926
- Kuulkers, E., den Hartog, P. R., in't Zand, J. J. M., Verbunt, F. W. M., Harris, W. E., & Cocchi, M., 2003, *A&A*, 399, 663
- Landolt, A. U., 1992, *AJ*, 104, 340
- Lattimer, J. M., & Prakash, M., 2004, *Science*, 304, 536
- Magnier, E., Lewin, W. H. G., van Paradijs, J., Tan, J., Penninx, W., & Damen, E., 1989, *MNRAS*, 237, 729
- McClintock, J., & Remillard, R., 2003, Review Article, *astro-ph/0306213*
- McClintock, J. E., Narayan, R., Garcia, M. R., Orosz, J. A., Remillard, R. A., & Murray, S. S., 2003, *ApJ*, 593, 435
- Menou, K., Esin, A. A., Narayan, R., Garcia, M. R., Lasota, J., & McClintock, J. E., 1999, *ApJ*, 520, 276
- Narayan, R., Garcia, M. R., & McClintock, J. E., 1997, *ApJ*, 478, L79
- Orosz, J. A., McClintock, J. E., Remillard, R. A., & Corbel, S., 2004, *ApJ*, 616, 376
- Parmar, A. N., White, N. E., Giommi, P., Stella, L., Sweeney, M., & Watson, M., 1985, *IAU Circular*, 4058
- Rutledge, R. E., Bildsten, L., Brown, E. F., Pavlov, G. G., Zavlin, V. E., & Ushomirsky, G., 2002, *ApJ*, 580, 413
- Taylor, B. G., Andresen, R. D., Peacock, A., & Zobl, R., 1981, *Space Science Reviews*, 30, 479
- Tomsick, J. A., et al., 2003, *ApJ*, 597, L133
- Tomsick, J. A., Gelino, D. M., Halpern, J. P., & Kaaret, P., 2004, *ApJ*, 610, 933
- Warwick, R. S., Norton, A. J., Turner, M. J. L., Watson, M. G., & Willingale, R., 1988, *MNRAS*, 232, 551
- Wijnands, R., 2004, *astro-ph/0405089*
- Wijnands, R., Heinke, C. O., & Grindlay, J. E., 2002, *ApJ*, 572, 1002
- Wijnands, R., Heinke, C. O., Pooley, D., Edmonds, P. D., Lewin, W. H. G., Grindlay, J. E., Jonker, P. G., & Miller, J. M., 2005a, *ApJ*, 618, 883
- Wijnands, R., Homan, J., Heinke, C. O., Miller, J. M., & Lewin, W. H. G., 2005b, *ApJ*, 619, 492
- Wijnands, R., Homan, J., Miller, J. M., & Lewin, W. H. G., 2004, *ApJ*, 606, L61
- Wijnands, R., Miller, J. M., Markwardt, C., Lewin, W. H. G., & van der Klis, M., 2001, *ApJ*, 560, L159
- Zavlin, V. E., Pavlov, G. G., & Shibanov, Y. A., 1996, *A&A*, 315, 141

TABLE 1
EXO 1747–214 X-RAY AND OPTICAL OBSERVATIONS

Start Time (UT)	Observatory	Instrument	Energy Band/Filter	Exposure Time (s)
1985 April 8, 2.3 h	<i>EXOSAT</i>	CMA	Thin Lexan ^a	869
1985 April 11, 10.0 h	<i>EXOSAT</i>	ME	1–20 keV	22,450
1985 April 11, 10.4 h	<i>EXOSAT</i>	CMA	Thin Lexan ^a	9,171
1985 April 11, 11.2 h	<i>EXOSAT</i>	CMA	Al/Parylene ^a	2,266
1985 April 11, 11.9 h	<i>EXOSAT</i>	CMA	Boron ^a	2,493
2002 February 24, 9.5 h	CTIO ^b	OSIRIS ^b	<i>J</i>	120
2003 July 31, 18.2 h	<i>Chandra</i>	ACIS-S	0.3–8 keV	24,479
2003 September 21, 5.9 h	Keck	ESI	<i>R</i>	600

^aThe three filters cover the 0.05–2.5 keV energy range with the different effective area curves described in the text.

^bWe used the 4 meter telescope at Cerro Tololo Inter-American Observatory with the OSIRIS (Optical System for Imaging and Low-Resolution Integrated Spectroscopy) instrument.